

Review

Fullerene Nanoarchitectonics with Shape-Shifting

Katsuhiko Ariga ^{1,2,*}  and Lok Kumar Shrestha ^{1,*} ¹ International Center for Materials Nanoarchitectonics (WPI-MANA),

National Institute for Materials Science (NIMS), 1-1 Namiki, Tsukuba 305-0044, Japan

² Graduate School of Frontier Sciences, The University of Tokyo, 5-1-5 Kashiwanoha, Kashiwa, Chiba 277-8561, Japan

* Correspondence: ARIGA.Katsuhiko@nims.go.jp (K.A.); SHRESTHA.Lokkumar@nims.go.jp (L.K.S.); Tel.: +81-029-860-4597 (K.A.); +81-029-860-4809 (L.K.S.)

Received: 22 April 2020; Accepted: 12 May 2020; Published: 15 May 2020



Abstract: This short review article introduces several examples of self-assembly-based structural formation and shape-shifting using very simple molecular units, fullerenes (C_{60} , C_{70} , and their derivatives), as fullerene nanoarchitectonics. Fullerene molecules are suitable units for the basic science of self-assembly because they are simple zero-dimensional objects with only a single elemental component, carbon, without any charged or interactive functional groups. In this review article, self-assembly of fullerene molecules and their shape-shifting are introduced as fullerene nanoarchitectonics. An outline and a background of fullerene nanoarchitectonics are first described, followed by various demonstrations, including fabrication of various fullerene nanostructures, such as rods on the cube, holes in the cube, interior channels in the cube, and fullerene micro-horns, and also a demonstration of a new concept, supramolecular differentiation.

Keywords: fullerene; interface; nanoarchitectonics; self-assembly; shape-shift

1. Introduction

There are social demands for innovations to solve various problems in energy production and storage [1,2], environmental protection and remediation [3,4], biomedical treatments [5,6], and sophisticated device innovations [7,8]. The primary approach of science and technology to answer these demands is the development of functional materials systems. Having good materials is one of the most necessary matters for the future development of human society.

Development of good materials systems is roughly divided into two steps. One of them is the synthesis of materials. This step includes organic synthesis of various chemicals [9–11], synthesis of functional polymers [12,13], and preparation of inorganic nano-materials [14–16] with their intrinsic high functions. Further materialization of these fundamental components into function-combined and/or function-advanced hybrids and composites [17,18] is also important. Further steps for materials development are structure regulations and construction of functional materials using synthesized molecular/nano units [19,20]. Micro-fabrication and nano-fabrication have brought innovations in materials structuring in recent decades [21,22]. In addition to various lithographic techniques, many kinds of nano-technological advancements enable us to observe, evaluate, and manipulate nano-scale objects, even including atoms and molecules.

Nano-technological procedures definitely lead to certain innovations in materials fabrication, but conventional chemical processes, such as self-assembly/self-organization [23,24], also have unavoidable contributions. Unlike nano-technology techniques under selected conditions, self-assembly processes can be applied universally to a wide range of molecular/nano units. Self-assembly to create specific materials from simple molecular units is a superior way to convert molecular-structure information to material-level information [25]. For example, well-defined structural regulation of one-dimensional

nano-tubes can be done through self-assembly of molecular units with well-designed interactive structures [26]. Extended supramolecular π -systems with specific color emissions are fabricated by self-assembly of borondipyrromethene (BODIPY) derivatives [27]. Because peptide molecules have structure-designable natures and high hydrogen bonding capabilities, they often become building blocks for self-assembly that are appropriate for materials fabrication in biomedical applications [28,29]. Recently, instructed assembly as self-assembly with a non-equilibrium process has been used for controls of living cell fates [30]. Although some unsolved problems remain in the basic science of self-assembly [31], self-assembling processes are widely used for the fabrication of functional materials with designed molecular units [32,33].

These two main research flows, developments in nano-technology and self-assembly in supramolecular chemistry, should be unified into one concept to fabricate functional materials systems from molecular/nano units with sufficient understanding of nano-level science. This task is assigned to an emerging concept, nanoarchitectonics (Figure 1) [34,35], as initially proposed by Masakazu Aono [36,37]. Nanoarchitectonics unifies nano-technology with the other scientific disciplines, such as supra-molecular chemistry, organic chemistry, nano-scale physics, and biology to architect functional materials systems from nano units. In the nanoarchitectonics process, functional materials are constructed with well-designed molecular/nano units through the combination and/or selection of various processes, including atom/molecular-level manipulation, chemical conversions by organic syntheses, self-assembly/self-organization, field-guided assemblies, micro/nano-fabrications, and biological processes [38,39]. The nanoarchitectonics concept mainly works on structural designs, but processes on functional designs are often included. Because this conceptual definition is rather ambiguous and acceptable for various materials systems, the nanoarchitectonics concept can be utilized for various research targets, such as materials synthesis [40,41], structural fabrication [42,43], catalysts [44,45], energy production and storage [46,47], environmental protection and remediation [48], sensors [49,50], sophisticated devices [51,52], biological investigations [53,54], and biomedical applications [55,56].

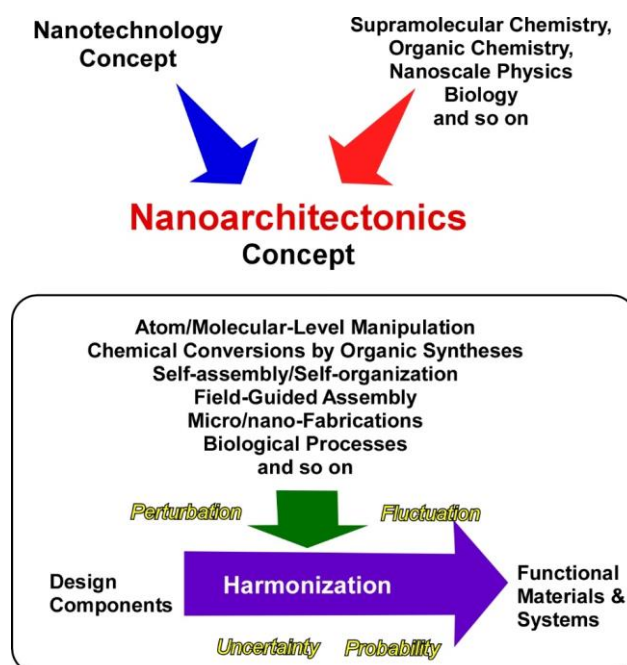


Figure 1. Outline of the nanoarchitectonics concept for the fabrication of functional materials and systems from molecular/nano units.

Unlike materials production in the macroscopic scale, materials architectonics in the nanoscopic scale cannot be simply done. In the nano-scale region, various uncertainties and complex natures,

including thermal fluctuations, statistical distributions, quantum effects, and complicated mutual component interactions have unavoidable influences in materials production processes. Fabrication of functional materials is not simply explained by the summation of individual effects, and harmonization of various events is rather necessary for the synthesis of functional materials [57]. Therefore, multiple steps and non-equilibrium processes can be included in materials production. The latter features are advantageous for fabrication of hierarchic structures [58], which cannot be easily achieved by conventional self-assembling processes.

In this short review article, we pick up fullerene molecules (C_{60} and C_{70}) as molecular units for the nanoarchitectonics processes to demonstrate high fabrication capabilities with structural variety from very simple units. Fullerene molecules and their derivatives are known as attractive structural units for electronic device systems [59] and solar cells [60]. In addition to their functional advantages, fullerene molecules are suitable units for the basic science of self-assembly. They are basically simple zero-dimensional objects with only a single elemental component, carbon, without any charged or interactive functional groups. In this review article, self-assembly of fullerene molecules and their shape-shifting are introduced as fullerene nanoarchitectonics. An outline and a background of fullerene nanoarchitectonics are first described, followed by various demonstrations, including fabrication of various structures, such as rods on the cube, holes in the cube, interior channels in the cube, and micro-horns, and also demonstration of a new concept, supramolecular differentiation.

2. Outline of Fullerene Nanoarchitectonics: Assembly and Shape-Shifts

Basic strategies for fullerene nanoarchitectonics with assembly and shape-shifts are briefly explained in this section. One of the key terms of these strategies is interface. Nanoarchitectonics processes, including self-assembly and dynamic functions at interfaces, have several specific features, such as restricted motional freedom, anisotropic structures, highly enhanced molecular interaction, and coupling of macroscopic dynamic motion and molecular functions [61–63]. Recent examples also show the importance of interfacial environments for various properties and functions as seen in surface domain controls through self-assembly of semi-fluorinated alkanes and related molecules [64], interface-regulated photoinduced motions of molecular arrays [65], the photocatalytic transformation of organic compounds upon surface complexation [66], heterogeneous low-temperature catalytic reactions upon surface protonics [67], and regulation of interfacial water for function design of polymeric biomaterials [68].

In the case of fullerene nanoarchitectonics, the interfacial process, so-called liquid-liquid interfacial precipitation (LLIP), has been especially used for fabrication of self-assembled structures with specific shapes (Figure 2) [69]. Although several methods for the fabrication of fullerene-based assembled materials, including slow evaporation of fullerene solutions, template synthesis, and vapor depositions, have been reported, the LLIP method has a versatile nature in fabrications of dimension-controlled fullerene assemblies from nano-scale to micro-scale. As a pioneer in fullerene assembly by the LLIP method, Miyazawa and co-workers have demonstrated mainly one-dimensional whiskers, rods, and tubes in well-regulated structural dimensions [70,71]. Not limited to typical one-dimensional structures, the LLIP method can be expanded to the fabrication of two-dimensional nanosheets, three-dimensional micro-cubes, ellipsoidal structures, and their modified structures.

The LLIP method is based on the difference in solubility of fullerene molecules between contacting two solvents. For example, fullerene molecules are first dissolved in a good solvent (with higher solubility), and then a poor solvent (with lower solubility) is added quickly to make a clear interface of these two liquids. This process is usually done with static and vibration-less conditions to produce fullerene assemblies with unified shapes. Shapes of the resulting fullerene assemblies are selected by a combination of good and poor solvents. Although the above-mentioned static-type LLIP processes are done with a rather long time (up to several days), the dynamic LLIP method described below utilized short-period processes for precipitation of fullerene assemblies with applying agitation actions, such as

handshaking, gentle sonication, and vortex motion. Formation of fullerene assemblies is quite quick, even occurring within a few minutes.

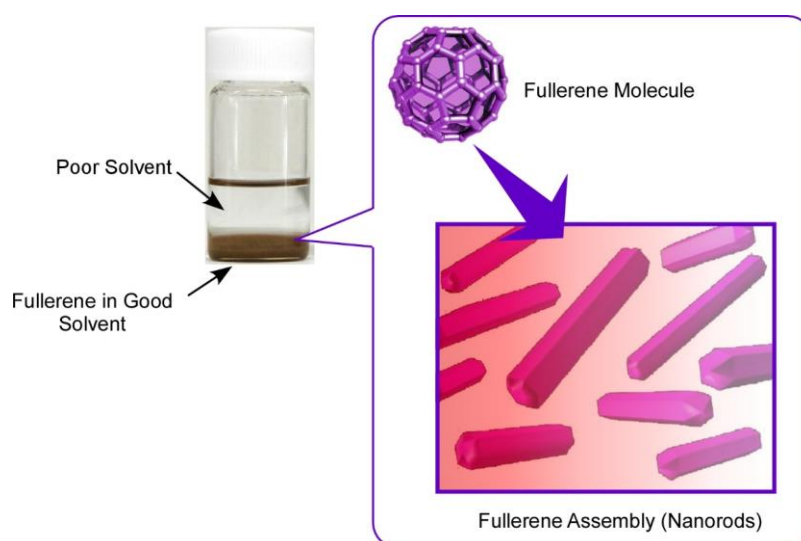


Figure 2. Liquid–liquid interfacial precipitation (LLIP) method for the fabrication of self-assembled structures with specific shapes.

At interfacial regions in the LLIP processes, the poor solvent diffused into the good solvent phase, lowering the solubility of fullerene molecules at the interfacial region. This process induces fullerene clusters (nucleus) formation, and further intermixing the solvents promotes the growth of fullerene assemblies. The LLIP processes include only simple action parameters, such as solvent combination, fullerene concentration, volume ratio of good solvent and poor solvent, temperature, and so on. Tuning of these parameters creates lots of possibilities to produce fullerene assemblies with various shapes and sizes according to our design and sometimes with unexpected surprises.

As mentioned in the following sections, exposing the formed fullerene assemblies to selected solvents can induce shape modification of the assemblies through surface dissolution and re-formation of another assembling structure. In addition, selective etching of the fullerene assemblies to make holes and channels is possible using some kinds of reagents, such as amine derivatives. These processes would work for shape-shifting of the preformed fullerene assemblies.

3. Examples of Fullerene Nanoarchitectonics: Assembly and Shape-Shifts

3.1. Rods on Cube

Hierarchic rods-on-cube structures of C_{60} assembly, where numerous rods attach to faces of the cubic structure, can be fabricated through shape-shifting from micro-cube structures prepared with C_{60} and $AgNO_3$ upon the LLIP method (Figure 3) [72]. The micro-cube structures were prepared via the LLIP method using a saturated solution of C_{60} in benzene or toluene and saturated solution of $AgNO_3$ in 1-butanol or 2-propanol. Micro-cubes were crystallized to sufficient size with edge lengths of 30–100 μm under static condition for 3 days to 1 week. The cubic motif was based on crystalline structures of C_{60} -Ag(I) organometallic hetero-nanostructure, $C_{60}(AgNO_3)_5$. A coordination network of silver(I) nitrate developed to form a zeolite-like motif and encapsulated C_{60} molecules. The fullerene–Ag(I) organometallic hetero-nanostructures were crystallized into micro-cubic structures at interfaces between benzene (or toluene) and 1-butanol (or 2-propanol).

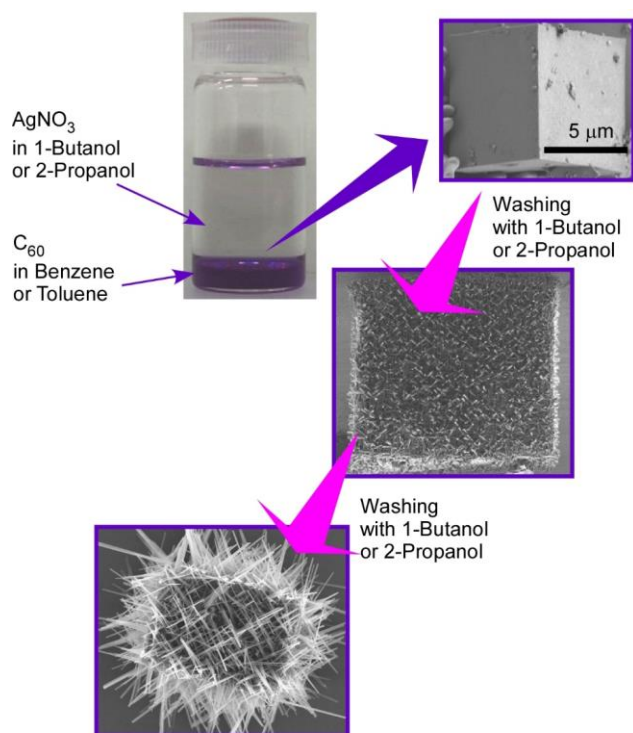


Figure 3. Hierarchic rods-on-cube structures of C_{60} assembly fabricated through shape-shifting from micro-cube structures prepared with C_{60} and $AgNO_3$ via the LLIP method.

Shape-shifting of the formed micro-cubes can be induced by exposure of the cubes with aliquots of small aliphatic alcohols, such as 1-butanol and 2-propanol. Smooth surfaces of cubes were transformed into surfaces with interpenetrated networks of rod-like crystals of pristine C_{60} . Interestingly, the orientation of the rod-like structures was determined by the orientation of the different crystal planes of the original micro-cubic crystals. The first washing of the original cubes with 1-butanol kept cubic shapes where rod-like structures ran along directions parallel to the face of the micro-cubes. Growth of the needles was enhanced by further washing of the cubes upon crystallization of C_{60} through the liberation of C_{60} molecules from C_{60} -Ag(I) organometallic hetero-nanostructure, $C_{60}(AgNO_3)_5$. Network structural growth of rod-like structures was more extended beyond the original cube dimension after three-times washing, and further washing destroyed the cube shapes to an assembly of nano-rods.

Transformation from cubic structures to rods-on-cube architectures is possible without using additional ions, such as silver ions in C_{70} assembly (Figure 4) [73]. In the latter case, the formation of cubic structures was done with a dynamic LLIP method. The cubic assembled structures were grown at the interface between C_{70} solution in mesitylene and *tert*-butyl alcohol with the aid of ultrasound application. Washing of the resulting micro-cubes with isopropyl alcohol at room temperature induced rearrangement of assembled structures into rods-on-cube architectures where nano-rods of C_{70} grew vertically from the face.

The formed hierarchic structures, rods-on-cube structures, have indeed a high surface area because of the presence of mesoporous structures (mesopore is defined as a pore with a diameter ranging from 2 to 50 nm) on the rod moieties. This feature is advantageous as sensing membranes for external gas substances. Sensor devices using quartz crystal micro-balances (QCM) modified with the synthesized rods-on-cube C_{70} assemblies were subjected to selective detections of chemical species in gas phases. The mesoporous rods work as a sensing antenna, especially for guest molecules. In addition to the high surface area nature, easy diffusion of gas molecules within mesopores on rods resulted in a high-sensing capability. Based on strong π - π interaction with C_{70} fullerene, the prepared sensor

systems exhibited selective sensitivity to aromatic guest molecules, such as benzene, pyridine, and toluene, which are considered to be experimentally toxic substances.

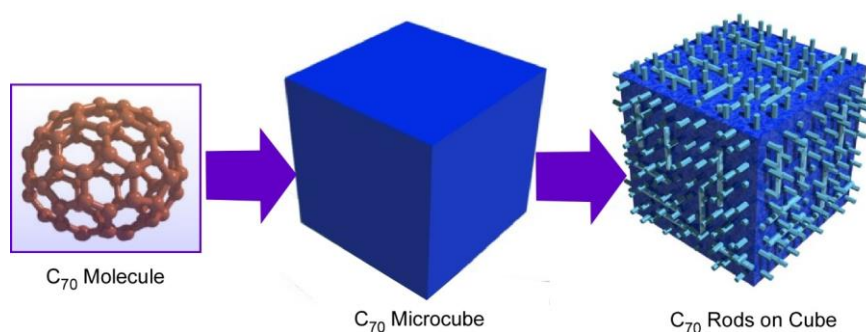


Figure 4. Hierarchic rods-on-cube structures of C_{60} assembly fabricated through shape-shifting from micro-cube structures prepared with C_{70} molecules.

3.2. Holes in Cube

Regulated porous nano-architectures, such as mesoporous materials [74,75], metal–organic frameworks [76,77], and related nano-porous structures [78,79], have been given much attention for various applications, such as facilitating sensing, drug delivery, and energy-related applications. By contrast, materials with regulated micro-porous structures are not so common. Size-defined micro-pores are useful for trapping toxic particles, such as PM2.5 particles (PM2.5: particle matters with a diameter of 2.5 μm or less) and undesirable bio-objects, such as virus particles and bacteria. Additionally, materials with such micro-pores can find application opportunities for encapsulation, protection, transport, and release of objects in micron and submicron size, such as various biomaterials.

Synthesis of micro-cubes of C_{70} molecules was performed with one regular micro-hole at the center of every face in the cubic structures (Figure 5) [80]. Shape-shifts for closure and re-opening of the micro-holes were demonstrated, together with selective trapping of micro-particles. Holes-in-cube architecture can be synthesized via the rapid LLIP method using *tert*-butyl alcohol and mesitylene as poor and good solvents, respectively. In this case, rapid addition of fullerene (C_{70}) solution into the poor solvents was unusually adopted. As is the typical procedure for holes-in-cube structures, C_{70} solution in mesitylene (1 mL, 1 mg/mL) was rapidly added into poor solvent of *tert*-butyl alcohol (3 mL). The resulting mixture was then incubated for 12 h at 25 $^{\circ}\text{C}$.

The holes formed at every face of micro-cubes can be intentionally closed though growing a thin fullerene sheet as a lid structure by adding excess C_{70} solution. Simple addition of C_{70} solution can cover almost all the open cubes. Thin films of C_{70} molecules were formed uniformly with thickness of ca. 700 nm. In addition, the resulting covered holes can be reopened by irradiation locally on the cube face using an electron beam (30 kV) for a short period (5–10 s). The thin lid layer of C_{70} was peeled off from the surface of cube faces to re-open the holes upon electron beam irradiation.

The holes-in-cube structures can discriminate carbon particles and polymer particles, although both of them have a hydrophobic nature, and their sizes are almost identical. In experiments to compare entrapment capabilities of graphitic carbon particles and resorcinol–formaldehyde polymeric resin particles, preferential capture of the former carbon particles over the latter resin particles was demonstrated based on microscopic observation by scanning electron microscopy (SEM: S-4800, Hitachi Co. Ltd. Tokyo, Japan). Most of the holes in the cubes of C_{70} molecules were occupied by the graphitic carbon particles, while entrapment of the resin particles was not so significant. The holes can preferentially entrap graphitic objects, probably due to surface π – π interaction. Although molecular-level recognition is a common subject [81,82], microscopic-level recognition for micron-sized particles has not been fully explored. The found example would open a novel category of microscopic materials recognition.

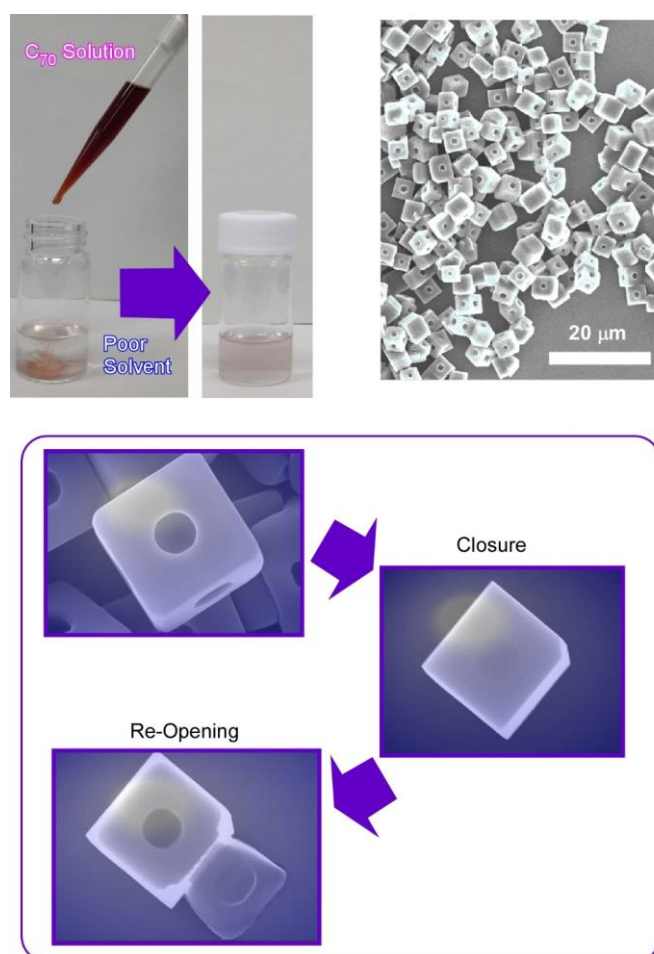


Figure 5. C_{70} holes-in-cube structure with one regular micro-hole at the center of every face in the cubic structures and its shape-shifts for closure and re-opening of the micro-hole.

3.3. Inside Etching

Shape-shifting of fullerene assemblies can be chemical etching using ethylene diamine for preformed assembling objects in different dimensions: one-dimensional C_{60} nano-rods, two-dimensional C_{60} nano-sheets, and three-dimensional C_{70} micro-cubes (Figure 6) [83]. Ethylene diamine is supposed to weakly react with fullerenes to form adducts, which have increased solubility for chemical etching. The chemical etching on one-dimensional C_{60} nano-rods occurred selectively from both ends of the nano-rods. The C_{60} nano-rods were shape-shifted into their hollow-structured nano-tubes. In the case of two-dimensional C_{60} nano-sheets, the etching is proceeded selectively from upper and bottom faces of the nano-sheets. To the three-dimensional micro-cube, the etching started from six faces of the micro-cubes, inducing shape-shifting from cubes into gyroid-like objects. These etched objects bear rather hydrophilic natures with increased dispersibility to aqueous phase. In addition, the etched fullerene objects with ethylene diamine exhibited high affinity to vapors of acids, such as formic acid and acetic acid. Selective sensors for these gas objects can be prepared by immobilizing the etched fullerene objects on QCM devices.

According to the post-shape-shifting procedure, fullerene micro-horns can be fabricated from fullerene micro-tubes of C_{60} and C_{70} mixture (Figure 7) [84]. In the first process, fullerene micro-tubes were fabricated via a dynamic LLIP method using C_{60}/C_{70} mesitylene (good solvent) solution and *tert*-butyl alcohol (bad solvent). Shape-shifting from micro-tubes to micro-horns occurred spontaneously upon addition of mixed solvent systems of mesitylene and *tert*-butyl alcohol and slow evaporation of the solvents. The resulting micro-horns had a sharp solid tip and hollow tubular end. The length of

the fullerene micro-horns (ca. 10 μm) was approximately half the length of the fullerene micro-tubes. Within the original micro-tubes, the concentration of C_{70} was decreased from the center to both ends. The addition of the mixed solvent system of good and poor solvents in a well-balanced ratio selectively etched the center of the micro-tube due to higher solubility of C_{70} over C_{60} . Interestingly, the fullerene micro-horns could selectively capture hydrophilic silica particles with a couple of hundred nanometers in diameter over the other particles in a similar size, such as fullerene particles and polystyrene latex particles. Therefore, the prepared micro-horn objects would be useful for the removal and sensing of biomaterials such as virus particles.

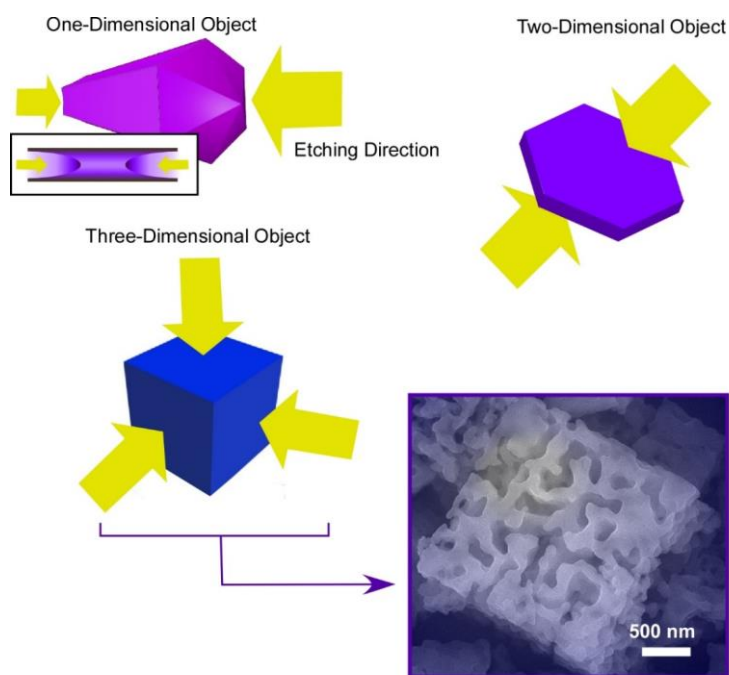


Figure 6. Chemical etching using ethylene diamine for preformed assembling objects in different dimensions: one-dimensional C_{60} nano-rods, two-dimensional C_{60} nano-sheets, and three-dimensional C_{70} micro-cubes.

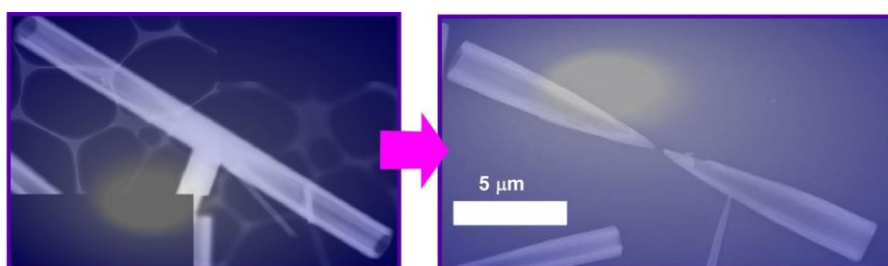


Figure 7. Fullerene micro-horns can be fabricated from fullerene micro-tubes of C_{60} and C_{70} mixture (these images are representative ones).

3.4. Supramolecular Differentiation

As the final example, a novel concept, supramolecular differentiation, is briefly explained. Living creatures can have a complicated organization from a single cell through a biologically important process of cellular differentiation. This process supports changes of non-specialized cells to more specialized types of cells. Differentiation progresses many times during the growth of multicellular organisms in response to the transformation of organisms to complex systems of tissue and cell types. Cellular differentiation induces drastic changes to shapes of living creatures, as seen in development

from eggs to tadpoles of frogs. The following example mimics such biological differentiation upon simple self-assembly of fullerene derivatives.

Self-assembly of two kinds of C_{60} derivatives, pentakis(phenyl)fullerene and pentakis-(4-dodecylphenyl)fullerene, at liquid–liquid interfacial media (2-propanol/toluene) induces supramolecular differentiation with the time-programmed regulation of multiple assembling processes (Figure 8) [85]. In the researched system, egg-like spherical assemblies were initially resulted at the liquid–liquid interface, and mixing two phases by external stimuli, such as gentle sonication, led to the growth of tails from the original eggs to form tadpole-like structures. The processes depend on the formation of phase-separated domains of pentakis-(4-dodecylphenyl)fullerene on the surface of the sphere made of pentakis(phenyl)fullerene. Differentiation to supramolecular tadpoles upon growth of tails made of pentakis-(4-dodecylphenyl)fullerene are only possible by mixing after the formation of phase-separated domains. The observed supramolecular differentiation could be regarded as an analogue of embryonic development in the field of material science.

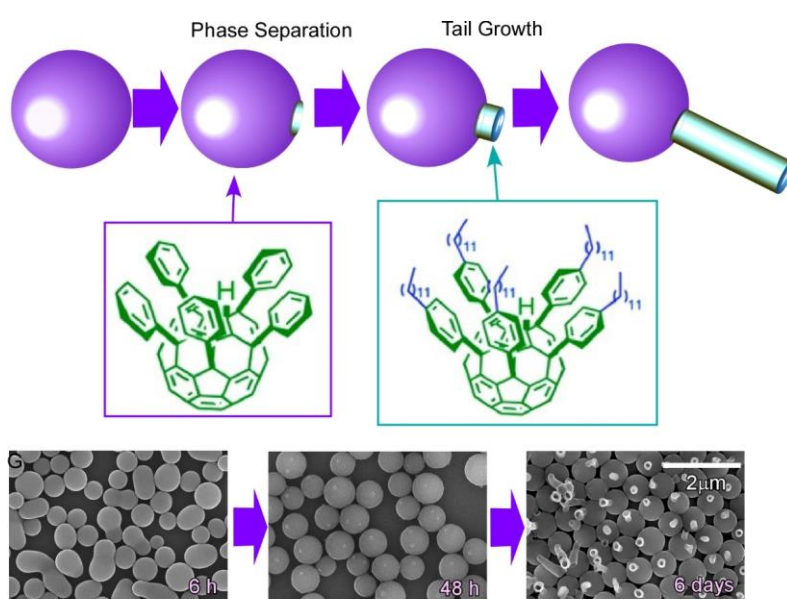


Figure 8. Supramolecular differentiation with the time-programmed regulation of multiple assembling processes.

4. Conclusions

This short review article introduces several examples of self-assembly-based structural formation and shape-shifting with using very simple molecular units, fullerenes (C_{60} , C_{70} , and their derivatives), as fullerene nanoarchitectonics. Even though using these unit components is so simple (basically single atom composition and zero-dimension), huge varieties of assembling objects can be obtained at liquid–liquid interfaces upon changing simple conditions, such as solvent compositions, concentrations, temperatures, and additional processes such as sonication. In addition, post-treatments, such as solvent washing and chemical etching, are useful for the production of hierarchic structures and integrated morphologies. It should be noted that all the processes can be done on a lab bench. Any expensive facilities such as lithography apparatuses and specific conditions such as high vacuum, ultra-low temperatures, and extremely clean conditions are not necessary. Molecular abilities for self-assembly and self-organization are capable of forming various architectures, even with high hierarchies. More advanced structure organization upon molecular-assembling capabilities can be commonly seen in biological systems where huge kinds of molecules are spontaneously organized into sophisticated structures under ambient conditions. The latter biological systems can be regarded as an ideal model for

materials science and nanoarchitectonics. From this viewpoint, novel challenges like supramolecular differentiations have to be more promoted.

In this review article, we just presented nanoarchitectonics examples of mainly simple fullerene derivatives. However, many experimental and theoretical approaches revealed various possibilities in functions and dynamic properties, together with the functionalization of fullerenes and their controlled assemblies [86–90]. Expanding the strategies described here to these wider candidates would create huge opportunities for function developments.

Although this review article shows rather limited application examples, fullerenes and their assemblies have various functional possibilities, as seen in bio-related applications and light energy conversion [91–94]. Possibilities in the practical application of nanoarchitected fullerene materials should be extended to a wider range of research fields, including energy, the environment, devices, and biomedical.

Funding: This work was partially supported by JSPS KAKENHI Grant Number JP16H06518 (Coordination Asymmetry), Grants-in-Aid for Scientific Research (A) Grant Number JP20H00392, and Grants-in-Aid for Scientific Research (C) Grant Number JP20K05590.

Conflicts of Interest: The authors declare no conflict of interest.

References

1. Guo, D.; Shibuya, R.; Akiba, C.; Saji, S.; Kondo, T.; Nakamura, J. Active sites of nitrogen-doped carbon materials for oxygen reduction reaction clarified using model catalysts. *Science* **2016**, *351*, 361–365. [[CrossRef](#)]
2. Miyasaka, T. Lead halide perovskites in thin film photovoltaics: Background and perspectives. *Bull. Chem. Soc. Jpn.* **2018**, *91*, 1058–1068. [[CrossRef](#)]
3. Fard, A.K.; McKay, G.; Buekenhoudt, A.; Al Sulaiti, H.; Motmans, F.; Khraisheh, M.; Atieh, M. Inorganic membranes: Preparation and application for water treatment and desalination. *Materials* **2018**, *11*, 74. [[CrossRef](#)]
4. Sai-Anand, G.; Sivanesan, A.; Benzigar, M.R.; Singh, G.; Gopalan, A.I.; Baskar, A.V.; Ilbeygi, H.; Ramadass, K.; Kambala, V.; Vinu, A. Recent progress on the sensing of pathogenic bacteria using advanced nanostructures. *Bull. Chem. Soc. Jpn.* **2019**, *92*, 216–244. [[CrossRef](#)]
5. Herbert, R.; Kim, J.H.; Kim, Y.S.; Lee, H.M.; Yeo, W.-H. Soft material-enabled, flexible hybrid electronics for medicine, healthcare, and human-machine interfaces. *Materials* **2018**, *11*, 187. [[CrossRef](#)] [[PubMed](#)]
6. Kobayashi, J.; Okano, T. Design of temperature-responsive polymer-grafted surfaces for cell sheet preparation and manipulation. *Bull. Chem. Soc. Jpn.* **2019**, *92*, 817–824. [[CrossRef](#)]
7. Alesanco, Y.; Vinuales, A.; Rodriguez, J.; Tena-Zaera, R. All-in-one gel-based electrochromic devices: Strengths and recent developments. *Materials* **2018**, *11*, 414. [[CrossRef](#)] [[PubMed](#)]
8. Watanabe, Y.; Sasabe, H.; Kido, J. Review of molecular engineering for horizontal molecular orientation in organic light-emitting devices. *Bull. Chem. Soc. Jpn.* **2019**, *92*, 716–728. [[CrossRef](#)]
9. Povie, G.; Segawa, Y.; Nishihara, T.; Miyauchi, Y.; Itami, K. Synthesis of a carbon nanobelt. *Science* **2017**, *356*, 172–175. [[CrossRef](#)]
10. Kawamura, S.; Sodeoka, M. Fluoroalkylation methods for synthesizing versatile building blocks. *Bull. Chem. Soc. Jpn.* **2019**, *92*, 1245–1262. [[CrossRef](#)]
11. Morisaki, Y.; Chujo, Y. Planar chiral [2.2]paracyclophanes: Optical resolution and transformation to optically active π -stacked molecules. *Bull. Chem. Soc. Jpn.* **2019**, *92*, 265–274. [[CrossRef](#)]
12. Gama, N.V.; Ferreira, A.; Barros-Timmons, A. Polyurethane foams: Past, present, and future. *Materials* **2018**, *11*, 1841. [[CrossRef](#)] [[PubMed](#)]
13. Akagi, K. Interdisciplinary chemistry based on integration of liquid crystals and conjugated polymers: Development and progress. *Bull. Chem. Soc. Jpn.* **2019**, *92*, 1509–1655. [[CrossRef](#)]
14. Novoselov, K.S.; Mishchenko, A.; Carvalho, A.; Castro Neto, A.H. 2D materials and van der Waals heterostructures. *Science* **2016**, *353*, aac9439. [[CrossRef](#)]
15. Maeda, K.; Mallouk, T.E. Two-dimensional metal oxide nanosheets as building blocks for artificial photosynthetic assemblies. *Bull. Chem. Soc. Jpn.* **2019**, *92*, 38–54. [[CrossRef](#)]

16. Rao, C.N.R.; Pramoda, K. Borocarbonitrides, BxCyNz, 2D nanocomposites with novel properties. *Bull. Chem. Soc. Jpn.* **2019**, *92*, 441–468. [[CrossRef](#)]
17. Pickering, K.L.; Efendy, M.G.A.; Le, T.M. A review of recent developments in natural fibre composites and their mechanical performance. *Compos. Pt. A-Appl. Sci. Manuf.* **2016**, *83*, 98–112. [[CrossRef](#)]
18. Sengottaiyan, C.; Jayavel, R.; Shrestha, R.G.; Subramani, T.; Maji, S.; Kim, J.H.; Hill, J.P.; Ariga, K.; Shrestha, L.K. Indium oxide carbon nanotube/reduced graphene oxide ternary nanocomposite with enhanced electrochemical supercapacitance. *Bull. Chem. Soc. Jpn.* **2019**, *92*, 521–528. [[CrossRef](#)]
19. Chen, G.; Roy, I.; Yang, C.; Prasad, P.N. Nanochemistry and nanomedicine for nanoparticle-based diagnostics and therapy. *Chem. Rev.* **2016**, *116*, 2826–2885. [[CrossRef](#)]
20. Imaoka, T.; Yamamoto, K. Wet-chemical strategy for atom-precise metal cluster catalysts. *Bull. Chem. Soc. Jpn.* **2019**, *92*, 941–948. [[CrossRef](#)]
21. Chen, C.-Y.; Wang, C.-M.; Liao, W.-S. A special connection between nanofabrication and analytical devices: Chemical lift-off lithography. *Bull. Chem. Soc. Jpn.* **2019**, *92*, 600–607. [[CrossRef](#)]
22. Kitamori, T. Thermal lens microscope and microchip chemistry. *Bull. Chem. Soc. Jpn.* **2019**, *92*, 469–473. [[CrossRef](#)]
23. Zhou, L.; Tan, Y.; Wang, J.; Xu, W.; Yuan, Y.; Cai, W.; Zhu, S.; Zhu, J. 3D self-assembly of aluminium nanoparticles for plasmon-enhanced solar desalination. *Nat. Photon.* **2016**, *10*, 393–398. [[CrossRef](#)]
24. Ariga, K.; Nishikawa, M.; Mori, T.; Takeya, J.; Shrestha, L.K.; Hill, J.P. Self-assembly as a key player for materials nanoarchitectonics. *Sci. Technol. Adv. Mater.* **2019**, *20*, 51–95. [[CrossRef](#)] [[PubMed](#)]
25. Komiyama, M.; Mori, T.; Ariga, K. Molecular imprinting: Materials nanoarchitectonics with molecular information. *Bull. Chem. Soc. Jpn.* **2018**, *91*, 1075–1111. [[CrossRef](#)]
26. Shimizu, T. Self-assembly of discrete organic nanotubes. *Bull. Chem. Soc. Jpn.* **2018**, *91*, 623–668. [[CrossRef](#)]
27. Cherumukkil, S.; Vedhanarayanan, B.; Das, G.; Praveen, V.K.; Ajayaghosh, A. Self-assembly of bodipy-derived extended π -systems. *Bull. Chem. Soc. Jpn.* **2018**, *91*, 100–120. [[CrossRef](#)]
28. Fukunaga, K.; Tsutsumi, H.; Mihara, H. Self-assembling peptides as building blocks of functional materials for biomedical applications. *Bull. Chem. Soc. Jpn.* **2019**, *92*, 391–399. [[CrossRef](#)]
29. Roy, B.; Govindaraju, T. Amino acids and peptides as functional components in arylenediimide-based molecular architectonics. *Bull. Chem. Soc. Jpn.* **2019**, *92*, 1883–1901. [[CrossRef](#)]
30. He, H.; Xu, B. Instructed-assembly (iA): A molecular process for controlling cell fate. *Bull. Chem. Soc. Jpn.* **2018**, *91*, 900–906. [[CrossRef](#)]
31. Hiraoka, S. Unresolved issues that remain in molecular self-assembly. *Bull. Chem. Soc. Jpn.* **2018**, *91*, 957–978. [[CrossRef](#)]
32. Boles, M.A.; Engel, M.; Talapin, D.V. Self-assembly of colloidal nanocrystals: from intricate structures to functional materials. *Chem. Rev.* **2016**, *116*, 11220–11289. [[CrossRef](#)] [[PubMed](#)]
33. Sawada, T.; Serizawa, T. Filamentous viruses as building blocks for hierarchical self-assembly toward functional soft materials. *Bull. Chem. Soc. Jpn.* **2018**, *91*, 455–466. [[CrossRef](#)]
34. Ariga, K.; Ji, Q.; Nakanishi, W.; Hill, J.P.; Aono, M. Nanoarchitectonics: A new materials horizon for nanotechnology. *Mater. Horiz.* **2015**, *2*, 406–413. [[CrossRef](#)]
35. Ariga, K.; Minami, K.; Ebara, M.; Nakanishi, J. What are emerging concepts and challenges in NANO?: Nanoarchitectonics, hand-operating nanotechnology, and mechanobiology. *Polym. J.* **2016**, *48*, 371–389. [[CrossRef](#)]
36. Ariga, K.; Ji, Q.; Hill, J.P.; Bando, Y.; Aono, M. Forming nanomaterials as layered functional structures towards materials nanoarchitectonics. *NPG Asia Mater.* **2012**, *4*, e17. [[CrossRef](#)]
37. Ariga, K.; Yamauchi, Y. Nanoarchitectonics from atom to life. *Chem. Asian. J.* **2020**, *15*, 718–728. [[CrossRef](#)]
38. Ariga, K.; Li, J.; Fei, J.; Ji, Q.; Hill, J.P. Nanoarchitectonics for dynamic functional materials from atomic/molecular-level manipulation to macroscopic action. *Adv. Mater.* **2016**, *28*, 1251–1286. [[CrossRef](#)]
39. Ariga, K.; Leong, D.T.; Mori, T. Nanoarchitectonics for hybrid and related materials for bio-oriented applications. *Adv. Funct. Mater.* **2018**, *28*, 1702905. [[CrossRef](#)]
40. Ramanathan, M.; Shrestha, L.K.; Mori, T.; Ji, Q.; Hill, J.P.; Ariga, K. Amphiphile nanoarchitectonics: From basic physical chemistry to advanced applications. *Phys. Chem. Chem. Phys.* **2013**, *15*, 10580–10611. [[CrossRef](#)]
41. Nakanishi, W.; Minami, K.; Shrestha, L.K.; Ji, Q.; Hill, J.P.; Ariga, K. Bioactive nanocarbon assemblies: Nanoarchitectonics and applications. *Nano Today* **2014**, *9*, 378–394. [[CrossRef](#)]

42. Rydzek, G.; Ji, Q.; Li, M.; Schaaf, P.; Hill, J.P.; Boulmedais, F.; Ariga, K. Electrochemical nanoarchitectonics and layer-by-layer assembly: from basics to future. *Nano Today* **2015**, *10*, 138–167. [[CrossRef](#)]
43. Ariga, K.; Mori, T.; Kitao, T.; Uemura, T. Supramolecular chiral nanoarchitectonics. *Adv. Mater.* **2020**, in press. [[CrossRef](#)] [[PubMed](#)]
44. Abe, H.; Liu, J.; Ariga, K. Catalytic nanoarchitectonics for environmentally-compatible energy generation. *Mater. Today* **2016**, *19*, 12–18. [[CrossRef](#)]
45. Wang, H.; Yin, S.; Eid, K.; Li, Y.; Xu, Y.; Li, X.; Xue, H.; Wang, L. Fabrication of mesoporous cage-bell Pt nanoarchitectonics as efficient catalyst for oxygen reduction reaction. *ACS Sus. Chem. Eng.* **2018**, *6*, 11768–11774. [[CrossRef](#)]
46. Xu, J.; Zhang, J.; Zhang, W.; Lee, C.-S. Interlayer nanoarchitectonics of two-dimensional transition-metal dichalcogenides nanosheets for energy storage and conversion applications. *Adv. Energy Mater.* **2017**, *7*, 1700571. [[CrossRef](#)]
47. Kim, J.; Kim, J.H.; Ariga, K. Redox active polymers for energy storage nanoarchitectonics. *Joule* **2017**, *1*, 739–768. [[CrossRef](#)]
48. Ariga, K.; Ishihara, S.; Abe, H.; Li, M.; Hill, J.P. Materials nanoarchitectonics for environmental remediation and sensing. *J. Mater. Chem.* **2012**, *22*, 2369–2377. [[CrossRef](#)]
49. Ishihara, S.; Labuta, J.; Van Rossom, W.; Ishikawa, D.; Minami, K.; Hill, J.P.; Ariga, K. Porphyrin-based sensor nanoarchitectonics in diverse physical detection modes. *Phys. Chem. Chem. Phys.* **2014**, *16*, 9713–9746. [[CrossRef](#)]
50. Pandeewar, M.; Senanayak, S.P.; Govindaraju, T. Nanoarchitectonics of small molecule and DNA for ultrasensitive detection of mercury. *ACS Appl. Mater. Interfaces* **2016**, *8*, 30362–30371. [[CrossRef](#)]
51. Ariga, K.; Ito, M.; Mori, T.; Watanabe, S.; Takeya, J. Atom/molecular nanoarchitectonics for devices and related applications. *Nano Today* **2019**, *28*, 100762. [[CrossRef](#)]
52. Ariga, K.; Ji, Q.; Mori, T.; Naito, M.; Yamauchi, Y.; Abe, H.; Hill, J.P. Enzyme nanoarchitectonics: Organization and device application. *Chem. Soc. Rev.* **2013**, *42*, 6322–6345. [[CrossRef](#)] [[PubMed](#)]
53. Zhao, L.; Zou, Q.; Yan, X. Self-assembling peptide-based nanoarchitectonics. *Bull. Chem. Soc. Jpn.* **2019**, *92*, 70–79. [[CrossRef](#)]
54. Liang, X.; Li, L.; Tang, J.; Komiyama, M.; Ariga, K. Dynamism of supramolecular DNA/RNA nanoarchitectonics: From interlocked structures to molecular machines. *Bull. Chem. Soc. Jpn.* **2020**, *93*, 581–603. [[CrossRef](#)]
55. Pandey, A.P.; Girase, N.M.; Patil, M.D.; Patil, P.O.; Patil, D.A.; Deshmukh, P.K. Nanoarchitectonics in cancer therapy and imaging diagnosis. *J. Nanosci. Nanotechnol.* **2014**, *14*, 828–840. [[CrossRef](#)]
56. Rozhina, E.; Ishmukhametov, I.; Batasheva, S.; Akhatova, F.; Fakhrullin, R. Nanoarchitectonics meets cell surface engineering: Shape recognition of human cells by halloysite-doped silica cell imprints. *Beilstein J. Nanotechnol.* **2019**, *10*, 1818–1825. [[CrossRef](#)]
57. Aono, M.; Ariga, K. The way to nanoarchitectonics & the way of nanoarchitectonics. *Adv. Mater.* **2016**, *28*, 989–992.
58. Ariga, K.; Jia, X.; Song, J.; Hill, J.P.; Leong, D.T.; Jia, Y.; Li, J. Nanoarchitectonics beyond self-assembly: Challenges to create bio-like hierarchic organization. *Angew. Chem. Int. Ed.* **2020**, in press. [[CrossRef](#)]
59. Akiyama, T. Development of fullerene thin-film assemblies and fullerene-diamine adducts towards practical nanocarbon-based electronic materials. *Bull. Chem. Soc. Jpn.* **2019**, *92*, 1181–1199. [[CrossRef](#)]
60. Yamane, S.; Suzuki, Y.; Mizukado, J. Photostability of poly(3-hexylthiophene) (P3HT) in P3HT:fullerene films: Effects of dispersed structures of fullerene derivatives. *Bull. Chem. Soc. Jpn.* **2018**, *91*, 1187–1192. [[CrossRef](#)]
61. Ariga, K.; Mori, T.; Hill, J.P. Mechanical control of nanomaterials and nanosystems. *Adv. Mater.* **2012**, *24*, 158–176. [[CrossRef](#)] [[PubMed](#)]
62. Ariga, K.; Yamauchi, Y.; Mori, T.; Hill, J.P. What can be done with the Langmuir-Blodgett method? Recent developments and its critical role in materials science. *Adv. Mater.* **2013**, *25*, 6477–6512. [[CrossRef](#)]
63. Ariga, K.; Mori, T.; Li, J. Langmuir nanoarchitectonics from basic to frontier. *Langmuir* **2019**, *35*, 3585–3599. [[CrossRef](#)] [[PubMed](#)]
64. Liu, X.; Riess, J.G.; Krafft, M.P. Self-organization of semifluorinated alkanes and related compounds at interfaces: Thin films, surface domains and two-dimensional spherulites. *Bull. Chem. Soc. Jpn.* **2018**, *91*, 846–857. [[CrossRef](#)]

65. Seki, T. Wide array of photoinduced motions in molecular and macromolecular assemblies at interfaces. *Bull. Chem. Soc. Jpn.* **2018**, *91*, 1026–1057. [[CrossRef](#)]
66. Leow, W.R.; Chen, X. Surface complexation for photocatalytic organic transformations. *Bull. Chem. Soc. Jpn.* **2019**, *92*, 505–510. [[CrossRef](#)]
67. Torimoto, M.; Murakami, K.; Sekine, Y. Low-temperature heterogeneous catalytic reaction by surface protonics. *Bull. Chem. Soc. Jpn.* **2019**, *92*, 1785–1792. [[CrossRef](#)]
68. Tanaka, M.; Kobayashi, S.; Murakami, D.; Aratsu, F.; Kashiwazaki, A.; Hoshiya, T.; Fukushima, K. Design of polymeric biomaterials: The “intermediate water concept”. *Bull. Chem. Soc. Jpn.* **2019**, *92*, 2043–2057. [[CrossRef](#)]
69. Shrestha, L.K.; Ji, Q.; Mori, T.; Miyazawa, K.; Yamauchi, Y.; Hill, J.P.; Ariga, K. Fullerene nanoarchitectonics: From zero to higher dimensions. *Chem. Asian J.* **2013**, *8*, 1662–1679. [[CrossRef](#)]
70. Miyazawa, K. Synthesis and properties of fullerene nanowhiskers and fullerene nanotubes. *J. Nanosci. Nanotechnol.* **2009**, *9*, 41–50. [[CrossRef](#)]
71. Miyazawa, K. Synthesis of fullerene nanowhiskers using the liquid-liquid interfacial precipitation method and their mechanical, electrical and superconducting properties. *Sci. Technol. Adv. Mater.* **2015**, *16*, 013502. [[CrossRef](#)]
72. Shrestha, L.K.; Sathish, M.; Hill, J.P.; Miyazawa, K.; Tsuruoka, T.; Sanchez-Ballester, N.M.; Honma, I.; Ji, Q.; Ariga, K. Alcohol-induced decomposition of Olmstead’s crystalline Ag(I)-fullerene heteronanostructure yields ‘Bucky cubes’. *J. Mater. Chem. C* **2013**, *1*, 1174–1181. [[CrossRef](#)]
73. Bairi, P.; Minami, K.; Nakanishi, W.; Hill, J.P.; Ariga, K.; Shrestha, L.K. Hierarchically-structured fullerene C₇₀ cube for sensing volatile aromatic solvent vapors. *ACS Nano* **2016**, *10*, 6631–6637. [[CrossRef](#)]
74. Li, W.; Liu, J.; Zhao, D. Mesoporous materials for energy conversion and storage devices. *Nat. Rev. Mater.* **2016**, *1*, 16023. [[CrossRef](#)]
75. Glotov, A.; Stavitskaya, A.; Chudakov, Y.; Ivanov, E.; Huang, W.; Vinokurov, V.; Zolotukhina, A.; Maximov, A.; Karakhanov, E.; Lvov, Y. Mesoporous metal catalysts templated on clay nanotubes. *Bull. Chem. Soc. Jpn.* **2019**, *92*, 61–69. [[CrossRef](#)]
76. Chaikittisilp, W.; Torad, N.L.; Li, C.; Imura, M.; Suzuki, N.; Ishihara, S.; Ariga, K.; Yamauchi, Y. Synthesis of nanoporous carbon-cobalt-oxide hybrid electrocatalysts by thermal conversion of metal-organic frameworks. *Chem. Eur. J.* **2014**, *20*, 4217–4221. [[CrossRef](#)] [[PubMed](#)]
77. Cui, Y.; Li, B.; He, H.; Zhou, W.; Chen, B.; Qian, G. Metal-organic frameworks as platforms for functional materials. *Acc. Chem. Res.* **2016**, *49*, 483–493. [[CrossRef](#)] [[PubMed](#)]
78. Liu, Q.; Wang, Y.; Dai, L.; Yao, J. Scalable fabrication of nanoporous carbon fiber films as bifunctional catalytic electrodes for flexible Zn-Air batteries. *Adv. Mater.* **2016**, *28*, 3000–3006. [[CrossRef](#)] [[PubMed](#)]
79. Azhar, A.; Li, Y.; Cai, Z.; Zakaria, M.B.; Masud, M.K.; Hossain, M.S.A.; Kim, J.; Zhang, W.; Na, J.; Yamauchi, Y.; et al. Nanoarchitectonics: A new materials horizon for Prussian blue and its analogues. *Bull. Chem. Soc. Jpn.* **2019**, *92*, 875–904. [[CrossRef](#)]
80. Bairi, P.; Minami, K.; Hill, J.P.; Ariga, K.; Shrestha, L.K. Intentional closing/opening of ‘hole-in-cube’ fullerene crystals with microscopic recognition properties. *ACS Nano* **2017**, *11*, 7790–7796. [[CrossRef](#)] [[PubMed](#)]
81. Ariga, K.; Ito, H.; Hill, J.P.; Tsukube, H. Molecular recognition: From solution science to nano/materials technology. *Chem. Soc. Rev.* **2012**, *41*, 5800–5835. [[CrossRef](#)] [[PubMed](#)]
82. Park, K.M.; Kim, J.; Ko, Y.H.; Ahn, Y.; Murray, J.; Li, M.; Shrinidhi, A.; Kim, K. Dye-cucurbit[n]uril complexes as sensor elements for reliable pattern recognition of biogenic polyamines. *Bull. Chem. Soc. Jpn.* **2018**, *91*, 95–99. [[CrossRef](#)]
83. Hsieh, C.-T.; Hsu, S.-h.; Maji, S.; Chahal, M.; Song, J.; Hill, J.P.; Ariga, K.; Shrestha, L.K. Post-assembly dimension-dependent face-selective etching of fullerene crystals. *Mater. Horiz.* **2020**, *7*, 787–795. [[CrossRef](#)]
84. Tang, Q.; Maji, S.; Jiang, B.; Sun, J.; Zhao, W.; Hill, J.P.; Ariga, K.; Fuchs, H.; Ji, Q.; Shrestha, L.K. Manipulating the structural transformation of fullerene microtubes to fullerene microhorns having microscopic recognition properties. *ACS Nano* **2019**, *13*, 14005–14012. [[CrossRef](#)]
85. Bairi, P.; Minami, K.; Hill, J.P.; Nakanishi, W.; Shrestha, L.K.; Liu, C.; Harano, K.; Nakamura, E.; Ariga, K. Supramolecular differentiation for constructing anisotropic fullerene nanostructures by time-programmed control of interfacial growth. *ACS Nano* **2016**, *10*, 8796–8802. [[CrossRef](#)]
86. Huber, S.E.; Gatchell, M.; Zettergren, H.; Mauracher, A. A precedent of van-der-Waals interactions outmatching Coulomb explosion. *Carbon* **2016**, *109*, 843–850. [[CrossRef](#)]

87. Cid, A.; Moldes, Ó.A.; Diniz, M.S.; Rodríguez-González, B.; Mejuto, J.C. Redispersion and Self-Assembly of C₆₀ Fullerene in Water and Toluene. *ACS Omega* **2017**, *2*, 2368–2373. [[CrossRef](#)]
88. Pankratyev, E.Y.; Tukhbatullina, A.A.; Sabirov, D.S. Dipole polarizability, structure, and stability of [2+2]-linked fullerene nanostructures (C₆₀)_n (n ≤ 7). *Phys. E* **2017**, *86*, 237–242. [[CrossRef](#)]
89. Vimalanathan, K.; Shrestha, R.G.; Zhang, Z.; Zou, J.; Nakayama, T.; Raston, C.L. Surfactant-free fabrication of fullerene C₆₀ nanotubes under shear. *Angew. Chem. Int. Ed.* **2017**, *56*, 8398–8401. [[CrossRef](#)]
90. Sabirov, D.S.; Garipova, R.R. The increase in the fullerene cage volume upon its chemical functionalization. *Fuller. Nanotub. Carbon Nanostruct.* **2019**, *27*, 702–709. [[CrossRef](#)]
91. Hasobe, T. Supramolecular nanoarchitectures for light energy conversion. *Phys. Chem. Chem. Phys.* **2010**, *12*, 44–57. [[CrossRef](#)] [[PubMed](#)]
92. Li, C.-Z.; Chueh, C.-C.; Yip, H.-L.; Ding, F.; Li, X.; Jen, A.K.-Y. Solution-processible highly conducting fullerenes. *Adv. Mater.* **2013**, *25*, 2457–2461. [[CrossRef](#)] [[PubMed](#)]
93. Wang, H.; Chen, Q.; Zhou, S. Carbon-based hybrid nanogels: A synergistic nanoplatform for combined biosensing, bioimaging, and responsive drug delivery. *Chem. Soc. Rev.* **2018**, *47*, 4198–4232. [[CrossRef](#)] [[PubMed](#)]
94. Taghavi, S.; Abnous, K.; Taghdisi, S.M.; Ramezani, M.; Alibolandi, M. Hybrid carbon-based materials for gene delivery in cancer therapy. *J. Control. Release* **2020**, *318*, 158–175. [[CrossRef](#)] [[PubMed](#)]



© 2020 by the authors. Licensee MDPI, Basel, Switzerland. This article is an open access article distributed under the terms and conditions of the Creative Commons Attribution (CC BY) license (<http://creativecommons.org/licenses/by/4.0/>).